Evidence for triplet superconductivity near an antiferromagnetic instability in CrAs

C. Y. Guo,[1] M. Smidman,[1,*] B. Shen,[1] W. Wu,[2] F. K. Lin,[1] X. L. Han,[2,3] Y. Chen,[1] F. Wu,[1] Y. F. Wang,[1] W. B. Jiang,[1] X. Lu,[1,4] J. P. Hu,[2,5] J. L. Luo,[2,5] and H. Q. Yuan[1,4,†]

[1]*Center for Correlated Matter and Department of Physics, Zhejiang University, Hangzhou 310058, China*
[2]*Beijing National Laboratory for Condensed Matter Physics and Institute of Physics, Chinese Academy of Sciences, Beijing 100190, China*
[3]*University of Chinese Academy of Sciences, Beijing 100049, China*
[4]*Collaborative Innovation Center of Advanced Microstructures, Nanjing University, Nanjing 210093, China*
[5]*Collaborative Innovation Center of Quantum Matter, Beijing 100871, China*

Superconductivity was recently observed in CrAs as the helimagnetic order is suppressed by applying pressure, suggesting possible unconventional superconductivity. To reveal the nature of the superconducting order parameter of CrAs, here we report the angular dependence of the upper critical field under pressure. Upon rotating the field by $360°$ in the bc plane, six maxima are observed in the upper critical field, where the oscillations have both sixfold- and twofold-symmetric components. Our analysis suggests the presence of an unconventional odd-parity spin-triplet state.

I. INTRODUCTION

Unconventional superconductivity, where the Cooper pairs are bound by a mechanism other than the conventional electron-phonon pairing mechanism described by BCS theory, has often been found to occur in close proximity to magnetic order in systems such as the cuprates, iron pnictides, and heavy-fermion superconductors. For instance, in many heavy-fermion materials, magnetism is suppressed to zero temperature at a quantum critical point (QCP) upon tuning with nonthermal parameters, which is often surrounded by a superconducting dome [1,2]. Non-Fermi-liquid behavior is observed in the quantum critical region, indicating the presence of strong critical spin fluctuations, which may mediate the unconventional superconductivity in these materials.

Recently, some other d-electron compounds have also been reported to show similar phase diagrams to the Ce-based heavy-fermion superconductors, namely, CrAs and MnP [3–5]. CrAs and MnP crystallize in an orthorhombic structure at room temperature, as displayed in Fig. 1(a). The room-temperature crystal structure corresponds to a distortion of the hexagonal NiAs-type structure with space group $P6_3/mmc$ and point group D_{6h} to the orthorhombic phase with space group $Pnma$ and point group D_{2h} [6]. The configuration of the Cr atoms in the undistorted hexagonal structure is displayed in Fig. 1(b), which is suggested to exist well above room temperature in CrAs [7], where two layers of hexagonally arranged Cr atoms are shown, with one Cr atom in the center. The arrangement of the Cr atoms after the orthorhombic distortion is shown in Fig. 1(c), where the hexagons are distorted along one direction in the layer. At ambient pressure, CrAs shows a first-order magnetic transition at $T_N = 265$ K

to a helimagnetic state, which occurs concurrently with a structural transition where there is an elongation of the b axis [7–10]. The ordering temperature T_N is suppressed upon applying pressure and vanishes above around 0.7 GPa [3,4], which likely coincides with the disappearance of the structural transition [10]. Meanwhile, superconductivity under pressure is also observed in the highest quality samples, where at lower pressures there is phase separation between superconductivity and magnetism, while at higher pressures T_N disappears and T_c reaches a maximum of around 2 K [3,4,11]. Evidence for spin fluctuations in the normal state was also found from the non-Fermi-liquid behavior of the resistivity with $\rho(T) \sim T^{1.5}$, as well as nuclear quadrupole resonance (NQR) measurements [12,13]. MnP also shows similar superconducting properties, where a superconducting dome is again observed after the suppression of magnetic order under pressure, which occurs at a higher pressure of around 8.0 GPa [5].

Another related family of Cr-based superconductors $A_2Cr_3As_3$ ($A =$ K, Rb, or Cs) [14–16] were recently reported with a hexagonal crystal structure (space group $P\bar{6}m2$). The structure shows some similarities to the undistorted hexagonal structure of CrAs, although rather than having a planar hexagonal arrangement, the Cr atoms form face-sharing octahedra. Despite the lack of long-range magnetic order, these materials also display a number of novel superconducting properties including very large and anisotropic upper critical fields [17–19], nodal superconducting order parameters [20–22], and low-dimensional spin fluctuations in the normal state [23,24]. It is therefore of particular interest to probe whether the superconductivity in CrAs and $A_2Cr_3As_3$ shares a common nature.

The characterization of pressure-induced superconductivity is experimentally challenging. Until now, very little is known about the superconducting gap symmetry and therefore the pairing mechanism of CrAs, even though its superconductivity appears on the border of antiferromagnetism. NQR

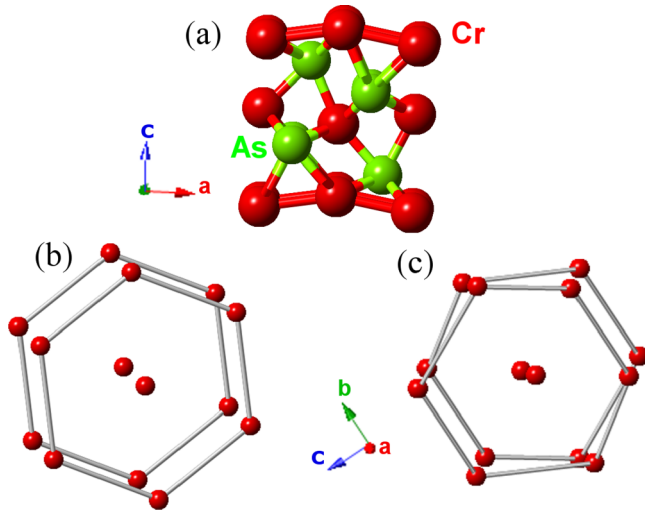*msmidman@zju.edu.cn
†hqyuan@zju.edu.cn

FIG. 1. (a) Unit cell of CrAs at room temperature with an orthorhombic structure, where Cr atoms are shown in red and As in green. The arrangement of the Cr atoms is shown for (b) the hexagonal NiAs-type structure and (c) the orthorhombic structure of CrAs which is a distortion of the aforementioned hexagonal structure.
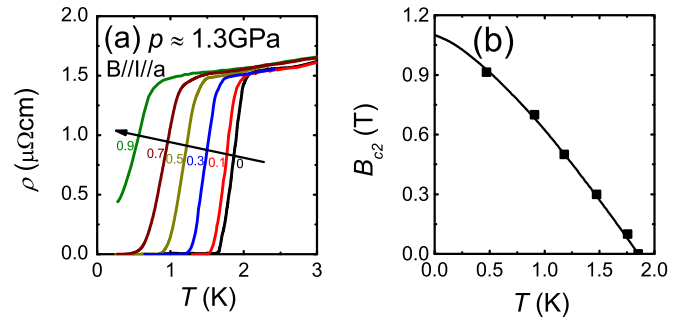

FIG. 2. (a) Temperature dependence of the electrical resistivity $\rho(T)$ at 1.3 GPa under various magnetic fields, with the field and current both applied parallel to the a axis. (b) Temperature dependence of the upper critical field $B_{c2}(T)$, determined from where there is a 50% drop of the resistivity relative to the normal state. The solid line shows a fit to an empirical formula described in the text.

measurements were performed under pressure at temperatures down to about 1 K ($\approx T_c/2$), which show that the temperature dependence of the spin-lattice relaxation rate $1/T_1$ lacks a coherence peak and follows a $\sim T^3$ dependence below T_c [12]. Although these results indicate unconventional superconductivity in CrAs with possible line nodes in the energy gap, its pairing state is still unclear and further characterization of the superconducting order parameter is badly needed. The field-angle dependence of quantities such as the upper critical field (B_{c2}) and heat capacity are powerful tools which can provide important information about the symmetry and structure of the superconducting gap [25–27]. Here, we report measurements of the angular dependence of B_{c2} of CrAs under pressure using a triple-axis vector magnet, in order to characterize the superconducting state of CrAs. We find a clear anisotropy of B_{c2} in the bc plane, where both twofold and sixfold oscillatory components are observed, which are consistent with an odd-parity triplet superconducting state.

II. EXPERIMENTAL DETAILS

Single crystals of CrAs were synthesized using Sn flux, as described previously [28]. The elements were combined in an atomic ratio Cr:As:Sn of 3:3:40, placed in an alumina crucible and sealed in an evacuated quartz ampoule. The ampoule was held at 650 °C for 8 h, then 1000 °C for 15 h, before being slowly cooled down to 600 °C and centrifuged. The needlelike single crystals, with the a axis along the needle direction are high quality, with a residual resistivity ratio at ambient pressure of $\rho(300\,\text{K})/\rho(2\,\text{K}) \approx 330$. Resistivity measurements under pressure were carried out using a piston-cylinder-type pressure cell, with Daphene 7373 used as a pressure transmitting medium to ensure hydrostaticity. The sample was mounted onto a rectangular plastic plate so that the needle axis of the sample was aligned with the long direction of the plate. The plate was then attached vertically to the plug of the pressure

cell. Although a small misalignment cannot be ruled out, this should not significantly affect our conclusions. The pressure was determined by measuring the superconducting transition of Pb. The angular dependence of the magnetoresistance was measured using a 370 resistive bridge with a triple-axis vector superconducting magnet that accommodates a ^{3}He cryostat. All the measurements were performed at one pressure of 1.3 GPa, with the current along the a axis.

III. RESULTS

A. Temperature and field-angle dependence of the resistivity

The temperature dependence of the resistivity [$\rho(T)$] of needle-shaped single crystals were measured with a current applied along the needle direction, which corresponds to the a axis. The measurements were performed at 1.3 GPa, well above the critical pressure for the suppression of magnetism and the structural transition, close to the pressure where the T_c is maximum and the normal state is paramagnetic. As shown in Fig. 2(a), a sharp superconducting transition is observed at about 1.85 K, slightly higher than reported previously [3]. The residual resistivity is about 1.5 $\mu\Omega$ cm, which is in good agreement with the former study and along with the sharp transition, indicates a high sample quality. Upon applying a field, the superconducting transition in $\rho(T)$ is suppressed to lower temperatures. The values of $B_{c2}(T)$ are determined from where $\rho(T)$ drops to 50% of the normal-state value, and are displayed in Fig. 2(b). The data are fitted using the empirical equation $B_{c2}(\text{T}) = B_{c2}(0)\{1 - [T/T_c]^n\}$, with $n = 1.36$. The extrapolated zero-temperature value $B_{c2}(0) = 1.1$ T is similar to the orbital limiting field [$B_{c2}^{orb}(0)$] of about 1.03 T calculated using $B_{c2}^{orb} = 0.72T_c(dB_{c2}/dT)_{T=T_c}$. This is compared to a Pauli limiting field of $B_P = 1.86T_c = 3.44$ T and corresponds to a Maki parameter $\alpha_M = \sqrt{2}B_{c2}^{orb}(0)/B_P$ of about $\alpha_M = 0.42$, which indicates that orbital pair breaking is the dominant pair-breaking mechanism in an applied magnetic field, and Pauli limiting is not expected to be significant. We also measured the resistivity upon rotating the applied magnetic field, so as to determine the angular dependence of B_{c2} at different temperatures. In Fig. 3, the resistivity is shown at three temperatures for various fields applied within
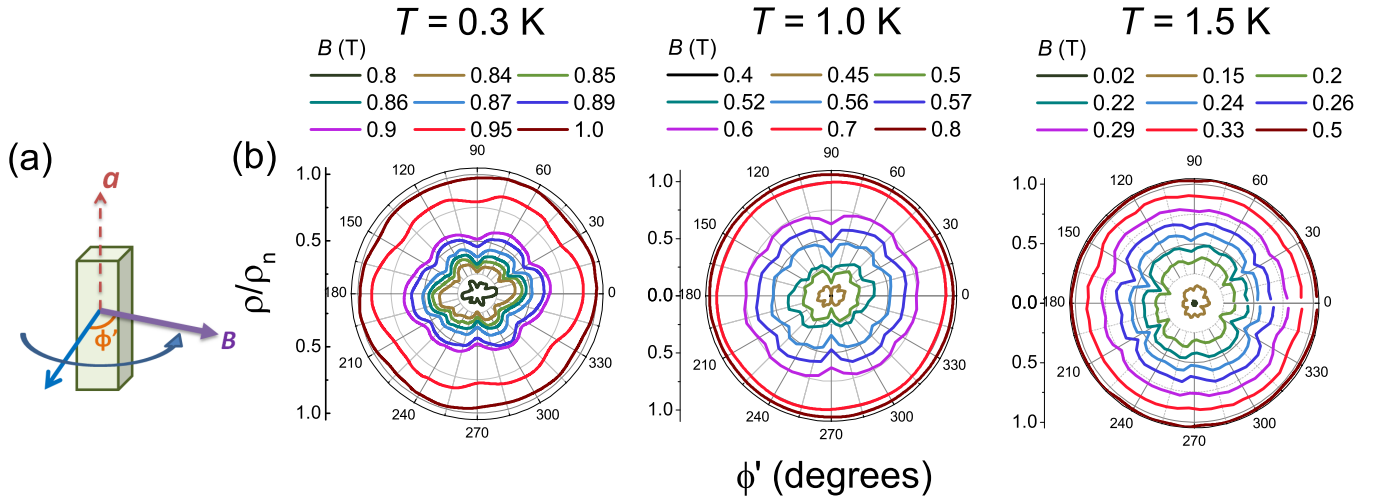
FIG. 3. (a) Illustration of the configuration for field-angle-dependent resistivity measurements. (b) Field-angle dependence of the electrical resistivity $\rho(\phi')$ for various magnetic fields applied within the bc plane at three temperatures, where the ϕ' is an azimuthal angle.

the bc plane, while the current was applied along the a axis, always perpendicular to the field direction. It can be seen that there are six dips of the resistivity upon rotating the field through 360°, which correspond to six maxima of B_{c2}.

B. Angle dependence of the upper critical field

The angular dependence of the upper critical field in the bc plane $[B_{c2}(\phi')]$ is shown in Fig. 4. Note that due to the thin needlelike shape of the single crystals, the position within the bc plane from which the azimuthal angle ϕ' is measured could not be determined, and therefore $\phi' = 0$ was chosen to correspond to where B_{c2} is at a minimum. The B_{c2} values were obtained by measuring $\rho(\phi')$ in various fields and taking the field where ρ is half the normal-state value, as displayed in Fig. 4(a). As shown in Fig. 4(b), at all temperatures there are six maxima in $B_{c2}(\phi')$ which are approximately separated by 60°. Overall, $B_{c2}(\phi')$ also shows the twofold symmetry of the orthorhombic crystal structure of CrAs and therefore these results suggest the presence of both sixfold- and twofold-symmetric components to the oscillations. There are also differences in the intensities of the peaks. At 0.3 K, the largest peaks are at about 90° and 270° and upon increasing the temperature to 1.0 K, the difference between the intensities of these two peaks and the others is enlarged. However, at 1.5 K, the peaks at 150° and 210° now have the greatest intensity, in contrast to the measurements at 0.3 and 1.0 K. This temperature is very close to T_c where the angular variation is much weaker, whereas at lower temperatures the anisotropy is much more pronounced. The presence of these sixfold and twofold components within the bc plane indicates that there is a non-s-wave pairing state. The out-of-plane angular dependence of the upper critical field as a function of the polar angle $[B_{c2}(\theta)]$ is shown in Fig. 5, where two large peaks can be observed rotating through 360°. The peak positions are at about 0° and 180°, which correspond to fields along the a axis.

The observation of an oscillatory $B_{c2}(\phi')$ gives evidence for unconventional superconductivity in CrAs. In the following, we discuss the potential superconducting states

compatible with this observation. We first derive the relation between the pairing symmetry and the angular dependence of the upper critical field H_{c2} based on Gorkov's theory [29–31]. Starting from a Hamiltonian with electron-electron interactions,

$$H = \sum_\sigma \int d^3\mathbf{r}\, \bar{\psi}_\sigma(\mathbf{r})\left(-\frac{\nabla^2}{2m} - \mu\right)\psi(\mathbf{r})$$
$$+ \int d^3\mathbf{r} \int d^3\mathbf{r}'\bar{\psi}_\uparrow(\mathbf{r})\bar{\psi}_\downarrow(\mathbf{r}')V(r - r')\psi_\downarrow(\mathbf{r}')\psi_\uparrow(\mathbf{r}),$$
$$(1)$$

where m and σ label the mass and spins of the electrons, respectively, the equations of motion can be written using the normal and anomalous Green's functions as

$$\left(i\omega_n - \frac{1}{2m}(-i\nabla + e\mathbf{A})^2\right)G_{\sigma,\sigma'}(\mathbf{r}, \mathbf{r}', \omega_n)$$
$$+ \sum_\rho \int d^3\xi\, \Delta_{\sigma\rho}(\mathbf{r}, \xi)\bar{F}_{\rho\sigma'}(\xi, \mathbf{r}', \omega_n) = \delta(\mathbf{r} - \mathbf{r}')\delta_{\sigma\sigma'},$$
$$(2)$$

$$\left(-i\omega_n - \frac{1}{2m}(-i\nabla - e\mathbf{A})^2\right)\bar{F}_{\sigma,\sigma'}(\mathbf{r}, \mathbf{r}', \omega_n)$$
$$+ \sum_\rho \int d^3\xi\, \Delta^*_{\sigma\rho}(\mathbf{r}, \xi)G_{\rho\sigma'}(\xi, \mathbf{r}', \omega_n) = 0 \qquad (3)$$

with the two Green's functions defined as

$$G_{\sigma\sigma'}(\mathbf{r}, \mathbf{r}', \tau) = -i\langle T_\tau(\psi_\sigma(\mathbf{r}, \tau)\bar{\psi}_{\sigma'}(\mathbf{r}', 0))\rangle,$$
$$F_{\sigma\sigma'}(\mathbf{r}, \mathbf{r}', \tau) = -i\langle T_\tau(\psi_\sigma(\mathbf{r}, \tau)\psi_{\sigma'}(\mathbf{r}', 0))\rangle \qquad (4)$$

in which $\psi(\tau) \equiv e^{H\tau}\psi(0)e^{-H\tau}$ is defined in the imaginary-time domain. The order parameter is given by $\Delta_{\sigma\sigma'}(\mathbf{r}, \mathbf{r}') = V(\mathbf{r} - \mathbf{r}')F_{\sigma\sigma'}(\mathbf{r}, \mathbf{r}')$. The free Green's function G^0 satisfies

$$\left(i\omega_n - \frac{1}{2m}(-i\nabla + e\mathbf{A})^2\right)G^0_{\sigma,\sigma'}(\mathbf{r}, \mathbf{r}', \omega_n)$$
$$= \delta(\mathbf{r} - \mathbf{r}')\delta_{\sigma\sigma'}. \qquad (5)$$

FIG. 5. Angular dependence of the upper critical field $B_{c2}(\theta)$ as a function of the polar angle θ, where $\theta = 0$ corresponds to the a axis.

with a solution

$$\overline{G}^0_{\sigma\sigma}(\mathbf{r}, \mathbf{r}', \omega_n) = -\frac{m}{2\pi |\mathbf{r} - \mathbf{r}'|}$$
$$\times \exp\left\{|\mathbf{r} - \mathbf{r}'|\left[ip_F \text{sgn}(\omega_n) - \frac{|\omega_n|}{v_F}\right]\right\}, \quad (9)$$

where p_F is the Fermi momentum. Upon plugging the above solution into Eq. (6) and considering the gap function in the center-of-mass coordinates and relative coordinates, we finally obtain the gap function

$$\Delta_{\sigma\sigma'}(\mathbf{R}, \mathbf{k}) = \int \frac{d^3\mathbf{k}'}{(2\pi)^3} TV(\mathbf{k} - \mathbf{k}')$$
$$\times \sum_{n,\rho} \int d^3\xi \, d^3\xi' e^{i\mathbf{k}'\cdot(\xi'-\xi)}$$
$$\times \overline{G}^0_{\sigma'\sigma'}(\xi, -\omega_n)e^{i\xi\cdot\Pi(\mathbf{R})}\Delta_{\sigma\rho}(\mathbf{R}, \mathbf{k}')$$
$$\times \overline{G}_{\rho\sigma'}(\mathbf{R}, \xi', \omega_n), \quad (10)$$

in which $\Pi(\mathbf{R}) \equiv -i\nabla + 2e\mathbf{A}(\mathbf{R})$ and $\Delta(\mathbf{R}, \mathbf{k}) = \int d^3\mathbf{r} \, e^{-i\mathbf{k}\cdot\mathbf{r}}\Delta(\mathbf{R}, \mathbf{r})$.

First, we take the in-plane p-wave pairing superconducting state [32–36] as an example, so as to derive the periodicity of H_{c2}. The p-wave order parameter is $\Delta(\mathbf{R}, \mathbf{k}) = \Delta(\mathbf{R})\cos(\phi)(|\uparrow\downarrow\rangle + |\downarrow\uparrow\rangle)/\sqrt{2}$, where ϕ is the azimuthal angle. In the weak coupling limit, Eq. (10) simplifies to

$$\Delta(\mathbf{R}) = gT \sum_n \int d^3\vec{\xi} \cos^2(\phi)\overline{G}^0_{\downarrow\downarrow}(\xi, -\omega_n)$$
$$\times \overline{G}^0_{\uparrow\uparrow}(\xi, \omega_n)e^{i\xi\cdot\Pi(\mathbf{R})}\Delta(\mathbf{R}), \quad (11)$$

where g is the interaction strength. By considering a magnetic field applied along the c axis, H_{c2} is determined by $\kappa\eta - \chi^*\chi = 0$, where

$$\kappa = 1 - gT \sum_n \int d^3\vec{\xi} \cos^2(\phi)\overline{G}^0_{\downarrow\downarrow}(\xi, -\omega_n)$$
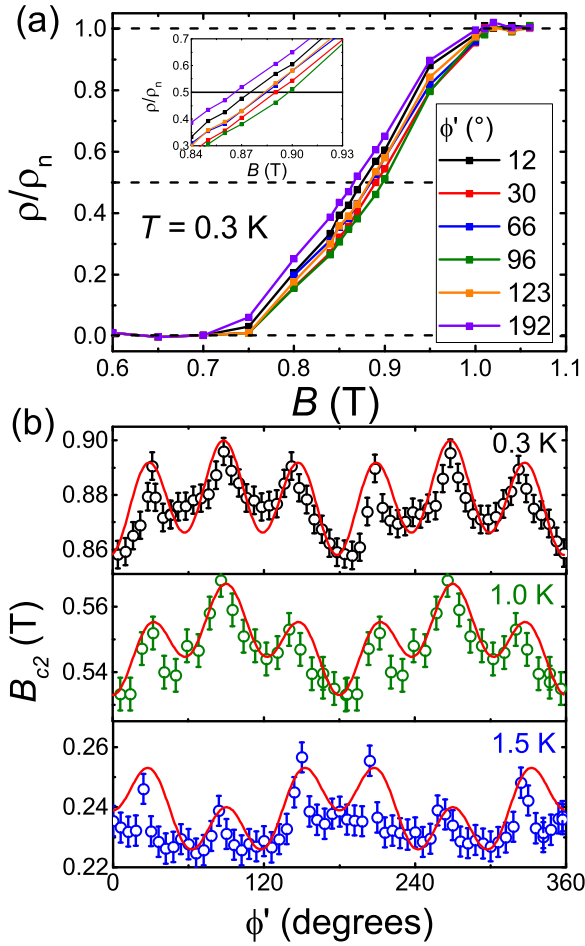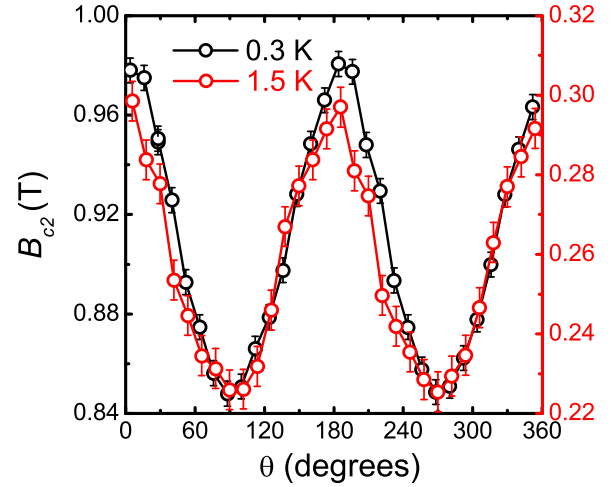$$\times \overline{G}^0_{\uparrow\uparrow}(\xi, \omega_n)e^{-\frac{eH_{c2}\xi^2}{2}}, \quad (12)$$

FIG. 4. (a) Determination of the upper critical field B_{c2} for different field angles ϕ' within the bc plane at 0.3 K, from the magnetic field dependence of the resistivity normalized by the normal-state value. The values of B_{c2} were taken from where the resistivity reaches half the normal-state value, as shown by the dashed line. The inset shows an enlargement of the data, in the vicinity of the upper critical fields. (b) Angular dependence of B_{c2} in the bc plane at 0.3, 1, and 1.5 K. The lines show the fits for the angular dependence of an odd-parity spin-triplet state with both twofold- and sixfold-symmetric components. The error bars are determined from the size of the field increments for the angle-dependent resistivity measurements.

From Eqs. (2) and (4) we obtain the gap equation as

$$\Delta_{\sigma\sigma'}(\mathbf{r}, \mathbf{r}') = TV(\mathbf{r} - \mathbf{r}')\sum_{n,\rho}\int d^3\xi \, d^3\xi' G^0_{\sigma'\sigma'}$$
$$\times (\mathbf{r}', \xi', -\omega_n)\Delta_{\sigma\rho}(\xi, \xi')G_{\rho\sigma'}(\mathbf{r}, \xi, \omega_n), \quad (6)$$

where T is the temperature and V is the interaction strength. In the presence of a magnetic field, we can further simplify the above equation by introducing

$$G(\mathbf{r}, \mathbf{r}') = e^{-ie\int_{\mathbf{r}'}^{\mathbf{r}} A(\mathbf{l})\cdot d\mathbf{l}}\overline{G}^0(\mathbf{r}, \mathbf{r}'), \quad (7)$$

and the corresponding $\overline{G}^0$, which satisfies

$$\left(i\omega_n - \frac{1}{2m}(-i\nabla)^2\right)\overline{G}^0_{\sigma,\sigma'}(\mathbf{r}, \mathbf{r}', \omega_n) = \delta(\mathbf{r} - \mathbf{r}')\delta_{\sigma\sigma'}, \quad (8)$$

$$\chi = -gT \sum_n \int d^3\vec{\xi}\, \cos^2(\phi) e^{2i\phi} \overline{G}_{\downarrow\downarrow}^0(\xi, -\omega_n)$$

$$\times \overline{G}_{\uparrow\uparrow}^0(\xi, \omega_n) e^{-\frac{eH_c\xi^2}{2}} \frac{eH_{c2}\xi^2 \sin^2\theta}{\sqrt{2}}, \qquad (13)$$

$$\eta = 1 - gT \sum_n \int d^3\vec{\xi}\, \cos^2(\phi) \overline{G}_{\downarrow\downarrow}^0(\xi, -\omega_n)$$

$$\times \overline{G}_{\uparrow\uparrow}^0(\xi, \omega_n) e^{-\frac{eH_c\xi^2}{2}} L_2(eH_{c2}\xi^2 \sin^2\theta). \qquad (14)$$

Here, θ is the polar angle and $L_2(x)$ is the second Laguerre polynomial, which is equal to $(x^2 - 4x + 2)/2$.

When there is an in-plane magnetic field at an angle θ_0 to the a axis, we can rotate the coordinates and rewrite the above equations by replacing $\cos^2(\phi)$ with the function

$$M(\theta_0, \vec{\xi}') = \frac{(-\sin\theta_0 \xi'_{y'} + \cos\theta_0 \xi'_{z'})^2}{(\xi')^2 - (\xi'_{z'})^2}, \qquad (15)$$

so that Eq. (11) becomes

$$\Delta(\mathbf{R}) = gT \sum_n \int d^3\vec{\xi}\, M(\theta_0, \vec{\xi}) \overline{G}_{\downarrow\downarrow}^0(\xi, -\omega_n)$$

$$\times \overline{G}_{\uparrow\uparrow}^0(\xi, \omega_n) e^{i\xi \cdot \Pi(\mathbf{R})} \Delta(\mathbf{R}). \qquad (16)$$

It is very clear from these equations that H_{c2} must be a function of $\cos(2\theta_0)$ and $\sin(2\theta_0)$, with an angular periodicity of π. Considering that the angular dependence is generally weak, we must have

$$H_{c2}(\theta_0) = H_{c2}^0 + \delta H_{c2} \cos(2\theta_0 + \alpha'), \qquad (17)$$

where α' is a constant for a given model.

The above result can immediately be extended to other pairing states. In general, if the superconducting order parameter has an in-plane gap function that is proportional to $\cos(n\phi_0)$, H_{c2} must have an angular period equal to $\frac{\pi}{n}$, namely,

$$H_{c2}(\theta_0) = H_{c2}^0 + \delta H_{c2} \cos(2n\theta_0 + \alpha'). \qquad (18)$$

The crystal structure of CrAs is orthorhombic with space group $Pnma$ and point group D_{2h}. As the orthorhombic distortion is rather small, we can characterize the superconducting properties by the $P6_3/mmc$ group together with a perturbative deviation caused by the orthorhombic distortion. Ignoring the distortion, the pairing symmetry should be classified by the D_{6h} point group. The hexagonal pattern of the in-plane anisotropy is consistent with the odd-parity spin-triplet f-wave pairing symmetry, which belongs to the B_{1u} or B_{2u} irreducible representation of D_{6h}. Assuming $\Delta(\mathbf{R}, \mathbf{k}) = \Delta(\mathbf{R})\Delta(\phi)(|\uparrow\downarrow\rangle + |\downarrow\uparrow\rangle)/\sqrt{2}$, and taking the B_{1u} gap function as an example, the specific gap function is proportional to $x(x^2 - 3y^2) = \cos(3\phi)$. Under such a pairing symmetry, the anisotropy of the in-plane B_{c2} is given by

$$B_{c2}(\phi') = \alpha + \beta \cos^2(3\phi'), \qquad (19)$$

which leads to a sixfold symmetry of the anisotropy following Eq. (18), where $\phi' = 0$ is chosen so that $\alpha' = 0$. We note that the only other pairing states compatible with the in-plane anisotropy are the spin-singlet B_{1g} or B_{2g} states. However, these higher-order pairings are expected to be energetically unfavorable, owing to the additional gapless region for $k_z = 0$.

Moreover, we can consider an orthorhombic distortion to the hexagonal structure where the point-group symmetry is lowered to D_{2h}, which corresponds to CrAs in the superconducting state. Taking the B_{1u} gap function $x(x^2 - 3y^2)$ under D_{6h}, both terms in $x(x^2 - 3y^2)$, namely, x^3 and xy^2, belong to B_{3u} under D_{2h}. Therefore, for the orthorhombic lattice, the lattice distortion can lead to the inclusion of a general symmetry-broken term as

$$\Delta(\phi) = x(x^2 - 3y^2) + \delta(x^3 + 3xy^2)$$

$$= \Delta_0 \cos(3\phi) + \delta \cos(\phi) + 2\delta \cos(\phi) \sin^2(\phi). \quad (20)$$

It is reasonable to neglect the last term in Eq. (20) since δ is much smaller than Δ_0. Thus, the pairing symmetry is approximately given by

$$\Delta(\phi) = \Delta_0 \cos(3\phi) + \delta \cos(\phi), \qquad (21)$$

which indicates that the superconducting state has a mixture of f- and p-wave pairing symmetries. Thus, the anisotropy of the in-plane B_{c2} can be generally written as

$$B_{c2}(\phi') = \alpha + \beta \cos^2(3\phi') + \gamma \cos^2(\phi'). \qquad (22)$$

As displayed in Fig. 4(b), this expression can account for the observed anisotropy in the bc plane, indicating that an odd-parity triplet superconducting state best explains the observed anisotropy. A similar modulation is obtained for the B_{2u} irreducible representation of D_{6h}, but since we cannot determine the crystallographic direction from which ϕ' is measured, we are unable to distinguish between the B_{1u} and B_{2u} states. At the lowest temperature, the sixfold component has a larger amplitude, with $\beta/\gamma \approx 3$, while at the higher temperatures they have comparable magnitudes with $\beta/\gamma \approx 1$.

The out-of-plane anisotropy in Fig. 5 can also be explained by assuming that the $S_z = \pm 1$ triplet pairing is slightly favored over $S_z = 0$ triplet pairing. In this case, the magnetic field parallel to the z direction does not cause the Zeeman splitting to break the Cooper pairs while an in-plane magnetic field has a strong Zeeman effect to break them. However, we also note that the maximum values correspond to fields parallel to the current, while the minima correspond to when the field and current are perpendicular. Since the Lorentz force exerted on vortices follows $\mathbf{H} \times \mathbf{I}$, where $\mathbf{H}$ and $\mathbf{I}$ are the applied fields and currents, this can lead to a lowering of the upper critical field measured using the resistivity and therefore may account for the out-of-plane anisotropy. On the other hand, the measurements in the bc plane were all performed with $\mathbf{H} \perp \mathbf{I}$ and therefore the effect of the Lorentz force cannot account for the in-plane anisotropy. We also note that although the hexagonal cross section of the needlelike single crystals may also give rise to a sixfold oscillation of the upper critical field due to demagnetization effects, this would require the system to have a significant magnetization. Since at the upper critical field the magnetization approaches the normal-state value, which likely corresponds to Pauli paramagnetism [37], and there is not a significant variation of the demagnetization factor within the bc plane, demagnetization effects do not account for the observed in-plane modulation. On the other hand, due to the thin needlelike shape of the sample, the change

of B_{c2} as a function of θ (Fig. 5) could have a contribution from demagnetization effects.

IV. DISCUSSION

The presence of an odd-parity spin-triplet state deduced from an oscillatory B_{c2} within the bc plane is also consistent with the evidence for line nodes and lack of coherence peak below T_c from NQR measurements [12]. Furthermore, the angular dependence of B_{c2} of CrAs is remarkably similar to that of $K_2Cr_3As_3$ [19], which shows a similar sixfold oscillation in the ab plane. This suggests f-wave pairing, which is one of the candidates proposed theoretically [38,39]. Therefore, the common features in the upper critical field and structural similarities between these Cr-based superconductors suggest a close relationship between the unconventional superconducting states of these materials, and that they may share a similar pairing mechanism. Moreover, there is evidence for spin fluctuations in the normal states of both compounds. In the case of $K_2Cr_3As_3$, both nuclear magnetic resonance and neutron scattering measurements indicate that there are short-range antiferromagnetic spin fluctuations [23,24]. Meanwhile the presence of spin fluctuations in CrAs is inferred from the low-temperature increase of $1/T_1T$ from NQR measurements, where the suppression of both $1/T_1T$ and T_c with increasing pressure suggests that an important role is played by spin fluctuations in the formation of superconductivity [12,13]. Together with our results, this could indicate the occurrence of triplet superconductivity mediated by antiferromagnetic spin fluctuations. This may be similar to the putative spin-triplet superconductor UPt_3, which also shows very weak antiferromagnetic order below $T_N = 5$ K [40–42], whereas antiferromagnetic correlations set in at higher temperatures [42,43]. Therefore, how such antiferromagnetic fluctuations can lead to a spin-triplet pairing state requires further experimental and theoretical exploration.

A further similarity between CrAs and UPt_3 is that both the undistorted hexagonal arrangement and the orthorhombic crystal structure of CrAs correspond to nonsymmorphic crystal structures. In the case of UPt_3, it was shown that nonsymmorphic symmetry allowed for the existence of triplet superconductivity with line nodes [44], and such symmetries have been shown more generally to lead to the topological protection of gap nodes [45]. Nonsymmorphic symmetries have also been found to lead to a variety of unusual topological states in condensed matter systems [46–48], and it was recently predicted that in UPt_3, the glide symmetry leads to a topological Möbius superconducting state with double Majorana cone surface states [49]. Meanwhile, a recent magnetotransport study of the normal state of CrAs found a nonsaturating linear magnetoresistance under pressure, which was suggested to originate from the topologically nontrivial band crossing protected by the nonsymmorphic symmetry [50]. Importantly, band structure calculations suggest that this novel band crossing is very close to Fermi level, and it is therefore of great interest to determine in future whether these topological features influence the superconductivity of CrAs. Furthermore, given that topological superconductivity has been proposed to occur in nodal spin-triplet superconductors, which can lead to unusual surface states [51], the possibility of its realization in CrAs due to our proposed triplet state with line nodes needs to be explored.

V. CONCLUSIONS

To summarize, we have measured the angular dependence of the upper critical field in the pressure-induced superconducting state of CrAs, which shows a sixfold oscillation in the bc plane. These findings are explained most naturally by an odd-parity spin-triplet pairing state. Furthermore, it is found that CrAs and $K_2Cr_3As_2$ display a similar angular dependence of the in-plane upper critical field, suggesting that these Cr-based superconductors may share a similar mechanism for the formation of superconductivity. Further experimental and theoretical investigations are necessary to reveal the unconventional pairing mechanism and explore the possibility of topological superconductivity in Cr-based superconductors.

[1] N. D. Mathur, F. M. Grosche, S. R. Julian, I. R. Walker, D. M. Freye, R. K. W. Haswelwimmer, and G. G. Lonzarich, Magnetically mediated superconductivity in heavy fermion compounds, Nature (London) **394**, 39 (1998).

[2] C. Pfleiderer, Superconducting phases of f-electron compounds, Rev. Mod. Phys. **81**, 1551 (2009).

[3] W. Wu, J. Cheng, K. Matsubayashi, P. Kong, F. Lin, C. Jin, N. Wang, Y. Uwatoko, and J. Luo, Superconductivity in the vicinity of antiferromagnetic order in CrAs, Nat. Commun. **5**, 5508 (2014).

[4] H. Kotegawa, S. Nakahara, H. Tou, and H. Sugawara, Superconductivity of 2.2 K under pressure in helimagnet CrAs, J. Phys. Soc. Jpn. **83**, 093702 (2014).

[5] J.-G. Cheng, K. Matsubayashi, W. Wu, J. P. Sun, F. K. Lin, J. L. Luo, and Y. Uwatoko, Pressure Induced Superconductivity on the Border of Magnetic Order in MnP, Phys. Rev. Lett. **114**, 117001 (2015).

[6] K. Motizuki, I. Hideaki, T. Itoh, and M. Morifuji, *Electronic Structure and Magnetism of 3d-Transition Metal Pnictides*, Springer Series in Materials Science (Springer, Berlin, 2009).

[7] H. Watanabe, N. Kazama, Y. Yamaguchi, and M. Ohashi, Magnetic structure of CrAs and Mn-substituted CrAs, J. Appl. Phys. **40**, 1128 (1969).

[8] K. Selte, A. Kjekshus, W. E. Jamison, A. F. Andresen, and J. E. Engebretsen, Magnetic structure and properties of CrAs, Acta Chem. Scand. **25**, 1703 (1971).

[9] L. Keller, J. S. White, M. Frontzek, P. Babkevich, M. A. Susner, Z. C. Sims, A. S. Sefat, H. M. Rønnow, and Ch. Rüegg, Pressure dependence of the magnetic order in CrAs: A neutron diffraction investigation, Phys. Rev. B **91**, 020409 (2015).

[10] Y. Shen, Q. Wang, Y. Hao, B. Pan, Y. Feng, Q. Huang, L. W. Harriger, J. B. Leao, Y. Zhao, R. M. Chisnell, J. W. Lynn, H. Cao, J. Hu, and J. Zhao, Structural and magnetic phase diagram of CrAs and its relationship with pressure-induced superconductivity, Phys. Rev. B **93**, 060503 (2016).

[11] R. Khasanov, Z. Guguchia, I. Eremin, H. Luetkens, A. Amato, P. K. Biswas, C. Rüegg, M. A. Susner, A. S. Sefat, N. D. Zhigadlo *et al.*, Pressure-induced electronic phase separation of magnetism and superconductivity in CrAs, Sci. Rep. **5**, 13788 (2015).

[12] H. Kotegawa, S. Nakahara, R. Akamatsu, H. Tou, H. Sugawara, and H. Harima, Detection of An Unconventional Superconducting Phase in the Vicinity of the Strong First-Order Magnetic Transition in CrAs Using ^{75}As-Nuclear Quadrupole Resonance, Phys. Rev. Lett. **114**, 117002 (2015).

[13] H. Kotegawa, K. Matsushima, S. Nakahara, H. Tou, J. Kaneyoshi, T. Nishiwaki, E. Matsuoka, H. Sugawara, and H. Harima, Superconductivity and magnetic fluctuations developing in the vicinity of strong first-order magnetic transition in CrAs, J. Phys.: Condens. Matter **29**, 234002 (2017).

[14] J.-K. Bao, J.-Y. Liu, C.-W. Ma, Z.-H. Meng, Z.-T. Tang, Y.-L. Sun, H.-F. Zhai, H. Jiang, H. Bai, C.-M. Feng, Z.-A. Xu, and G.-H. Cao, Superconductivity in Quasi-One-Dimensional $K_2Cr_3As_3$ with Significant Electron Correlations, Phys. Rev. X **5**, 011013 (2015).

[15] Z.-T. Tang, J.-K. Bao, Y. Liu, Y.-L. Sun, A. Ablimit, H.-F. Zhai, H. Jiang, C.-M. Feng, Z.-A. Xu, and G.-H. Cao, Unconventional superconductivity in quasi-one-dimensional $Rb_2Cr_3As_3$, Phys. Rev. B **91**, 020506 (2015).

[16] Z.-T. Tang, J.-K. Bao, Z. Wang, H. Bai, H. Jiang, Y. Liu, H.-F. Zhai, C.-M. Feng, Z.-A. Xu, and G.-H. Cao, Superconductivity in quasi-one-dimensional $Cs_2Cr_3As_3$ with large interchain distance, Sci. China Mater. **58**, 16 (2015).

[17] T. Kong, S. L. Bud'ko, and P. C. Canfield, Anisotropic H_{c2}, thermodynamic and transport measurements, and pressure dependence of T_c in $K_2Cr_3As_3$ single crystals, Phys. Rev. B **91**, 020507 (2015).

[18] F. F. Balakirev, T. Kong, M. Jaime, R. D. McDonald, C. H. Mielke, A. Gurevich, P. C. Canfield, and S. L. Bud'ko, Anisotropy reversal of the upper critical field at low temperatures and spin-locked superconductivity in $K_2Cr_3As_3$, Phys. Rev. B **91**, 220505 (2015).

[19] H. Zuo, J.-K. Bao, Y. Liu, J. Wang, Z. Jin, Z. Xia, L. Li, Z. Xu, J. Kang, Z. Zhu, and G.-H. Cao, Temperature and angular dependence of the upper critical field in $K_2Cr_3As_3$, Phys. Rev. B **95**, 014502 (2017).

[20] G. M. Pang, M. Smidman, W. B. Jiang, J. K. Bao, Z. F. Weng, Y. F. Wang, L. Jiao, J. L. Zhang, G. H. Cao, and H. Q. Yuan, Evidence for nodal superconductivity in quasi-one-dimensional $K_2Cr_3As_3$, Phys. Rev. B **91**, 220502 (2015).

[21] D. T. Adroja, A. Bhattacharyya, M. Telling, Yu. Feng, M. Smidman, B. Pan, J. Zhao, A. D. Hillier, F. L. Pratt, and A. M. Strydom, Superconducting ground state of quasi-one-dimensional $K_2Cr_3As_3$ investigated using μSR measurements, Phys. Rev. B **92**, 134505 (2015).

[22] J. Yang, Z. T. Tang, G. H. Cao, and Guo-qing Zheng, Ferromagnetic Spin Fluctuation and Unconventional Superconductivity in $Rb_2Cr_3As_3$ Revealed by ^{75}As NMR and NQR, Phys. Rev. Lett. **115**, 147002 (2015).

[23] H. Z. Zhi, T. Imai, F. L. Ning, J.-K. Bao, and G.-H. Cao, NMR Investigation of the Quasi-One-Dimensional Superconductor $K_2Cr_3As_3$, Phys. Rev. Lett. **114**, 147004 (2015).

[24] K. M. Taddei, Q. Zheng, A. S. Sefat, and C. de la Cruz, Coupling of structure to magnetic and superconducting orders in quasi-one-dimensional $K_2Cr_3As_3$, Phys. Rev. B **96**, 180506(R) (2017).

[25] H. A. Vieyra, N. Oeschler, S. Seiro, H. S. Jeevan, C. Geibel, D. Parker, and F. Steglich, Determination of Gap Symmetry from Angle-Dependent H_{c2} Measurements on $CeCu_2Si_2$, Phys. Rev. Lett. **106**, 207001 (2011).

[26] F. Weickert, P. Gegenwart, H. Won, D. Parker, and K. Maki, In-plane angular dependence of the upper critical field in $CeCoIn_5$, Phys. Rev. B **74**, 134511 (2006).

[27] K. An, T. Sakakibara, R. Settai, Y. Onuki, M. Hiragi, M. Ichioka, and K. Machida, Sign Reversal of Field-Angle Resolved Heat Capacity Oscillations in a Heavy Fermion Superconductor $CeCoIn_5$ and $d_{x^2-y^2}$ Pairing Symmetry, Phys. Rev. Lett. **104**, 037002 (2010).

[28] Wei Wu, XiaoDong Zhang, ZhiHua Yin, Ping Zheng, NanLin Wang, and JianLin Luo, Low temperature properties of pnictide CrAs single crystal, Sci. China **53**, 1207 (2010).

[29] L. P. Gor'kov, Microscopic derivation of the Ginzburg-Landau equations in the theory of superconductivity, Sov. Phys. JETP **9**, 1364 (1959).

[30] E. Helfand and N. R. Werthamer, Temperature and purity dependence of the superconducting critical field, H_{c2}. II, Phys. Rev. **147**, 288 (1966).

[31] I. A. Luk'yanchuk and V. P. Mineev, Upper critical fields in p-pairing superconductors, Sov. Phys. JETP **66**, 1168 (1987).

[32] A. A. Abrikosov, On the magnetic properties of superconductors of the second group, Sov. Phys. JETP **5**, 1174 (1957).

[33] K. Scharnberg and R. A. Klemm, p-wave superconductors in magnetic fields, Phys. Rev. B **22**, 5233 (1980).

[34] K. Scharnberg and R. A. Klemm, Upper Critical Field in p-Wave Superconductors with Broken Symmetry, Phys. Rev. Lett. **54**, 2445 (1985).

[35] M. Prohammer and J. P. Carbotte, Upper critical field of s- and d-wave superconductors with anisotropic effective mass, Phys. Rev. B **42**, 2032 (1990).

[36] D. Chang, C.-Y. Mou, B. Rosenstein, and C. L. Wu, Static and dynamical anisotropy effects in the mixed state of d-wave superconductors, Phys. Rev. B **57**, 7955 (1998).

[37] T. Suzuki and H. Ido, Magnetic-nonmagnetic transition in CrAs and the related compounds, J. Appl. Phys. **73**, 5686 (1993).

[38] Y. Zhou, C. Cao, and F.-C. Zhang, Theory for superconductivity in alkali chromium arsenides $A_2Cr_3As_3$ (A = K, Rb, Cs), Sci. Bull. **62**, 208 (2017).

[39] X. Wu, F. Yang, C. Le, H. Fan, and J. Hu, Triplet p_z-wave pairing in quasi-one-dimensional $A_2Cr_3As_3$ superconductors (A = K, Rb, Cs), Phys. Rev. B **92**, 104511 (2015).

[40] R. H. Heffner, D. W. Cooke, A. L. Giorgi, R. L. Hutson, M. E. Schillaci, H. D. Rempp, J. L. Smith, J. O. Willis, D. E. MacLaughlin, C. Boekema, R. L. Lichti, J. Oostens, and A. B. Denison, Muon spin rotation in the magnetic and superconducting ground states of $(U,Th)Be_{13}$ and $(U,Th)Pt_3$, Phys. Rev. B **39**, 11345 (1989).

[41] G. Aeppli, E. Bucher, C. Broholm, J. K. Kjems, J. Baumann, and J. Hufnagl, Magnetic Order and Fluctuations in Superconducting UPt_3, Phys. Rev. Lett. **60**, 615 (1988).

[42] R. Joynt and L. Taillefer, The superconducting phases of UPt_3, Rev. Mod. Phys. **74**, 235 (2002).

[43] G. Aeppli, E. Bucher, A. I. Goldman, G. Shirane, C. Broholm, and J. K. Kjems, Magnetic correlations in UPt_3 and $U_{1-x}Th_xPt_3$, J. Magn. Magn. Mater. **76**, 385 (1988).

[44] M. R. Norman, Odd parity and line nodes in heavy-fermion superconductors, Phys. Rev. B **52**, 15093 (1995).

[45] S. Kobayashi, Y. Yanase, and M. Sato, Topologically stable gapless phases in nonsymmorphic superconductors, Phys. Rev. B **94**, 134512 (2016).

[46] Z. Wang, A. Alexandradinata, R. J. Cava, and B. Andrei Bernevig, Hourglass fermions, Nature (London) **532**, 189 (2016).

[47] J. Ma, C. Yi, B. Lv, ZhiJun Wang, S. Nie, L. Wang, L. Kong, Y. Huang, P. Richard, P. Zhang *et al.*, Experimental evidence of hourglass fermion in the candidate nonsymmorphic topological insulator KHgSb, Sci. Adv. **3**, e1602415 (2017).

[48] Po-Yao Chang, O. Erten, and P. Coleman, Mobius Kondo insulators, Nat. Phys. **13**, 794 (2017).

[49] Y. Yanase and K. Shiozaki, Möbius topological superconductivity in UPt_3, Phys. Rev. B **95**, 224514 (2017).

[50] Q. Niu, W. C. Yu, K. Y. Yip, Z. L. Lim, H. Kotegawa, E. Matsuoka, H. Sugawara, H. Tou, Y. Yanase, and S. K. Goh, Quasilinear quantum magnetoresistance in pressure-induced nonsymmorphic superconductor chromium arsenide, Nat. Commun. **8**, 15358 (2017).

[51] A. P. Schnyder and P. M. R. Brydon, Topological surface states in nodal superconductors, J. Phys.: Condens. Matter **27**, 243201 (2015).